Reaction Mechanism.—Based on the similarity of the octahedral hexaaquo ions that are the predominant species for V(II) and V(III) and the structural similarities of the oxo ions that are the predominant V(IV) and V(V) species, it seems most likely that in reaction I V^{2+} is converted to V^{3+} and VO_2^+ to VO^{2+}. This conclusion might be checked with the appropriate radiotracer experiments, but these were not done. Mild support for this assertion also comes from the general preference for one-electron over two-electron changes shown by reactions in which either would be allowed by reason of the stability of the intermediate oxidation states. The very low rate of electron exchange[7] between V^{3+} and VO^{2+}, the products of the reaction in question, also lends support to the conclusion that this is not a two-electron process because in such an exchange (in contrast to the V^{2+}–V^{3+} and VO^{2+}–VO_2^+ reaction) interconversion of aquo and oxo ions is needed.

The information contained in the present results does not allow any firm conclusions concerning structural features of the transition states to be drawn. Some features of the detailed mechanism are evident, however. If a hydroxo or oxo anion acts as a bridging group for electron transfer, it is derived from a solvent molecule coordinated to V(II), since the exchange rate of $V(H_2O)_6^{2+}$ and bulk water occurs too slowly to permit either pathway to involve displacement of a V(II) water ligand.[27]

The surprisingly negative value of $S^{\pm}$ for the transition state of 3+ charges in VII may reflect the retention in the transition state of *all* of the coordinated solvent molecules.[28] The addition of a proton in the second pathway is a common occurrence[26,29] in reactions where the net structural change converts an oxo ligand to an aquo ligand (*e.g.*, VO_2^+ to VO^{2+}), presumably because the additional proton, by coordination to a VO_2^+ oxygen in the transition state, assists in its conversion into a water molecule. An appropriate concerted motion of protons could give the inner-sphere transition state $[(H_2O)_5V(OH)V(O)(H_2O)_n^{4+}]^{\pm}$, but the results do not provide a clear indication on this point.

(27) The rate constant for the $V(H_2O)_6^{2+}$–H_2O exchange rate is not known, but the rate constant for anation of $V(H_2O)_6^{2+}$ by SCN^- is 28 M^{-1} sec^{-1},[21] and one can infer from similar comparisons [N. Sutin, *Ann. Rev. Phys. Chem.*, **17**, 119 (1966)] that the solvent rate is probably less than 10-fold higher.

(28) An abnormally positive value of $\Delta S^{\pm}$ was used to infer an inner-sphere mechanism: M. J. Nicol and D. R. Rosseinsky, *Chem. Ind.* (London), 1166 (1963). T. W. Newton and F. B. Baker, *J. Phys. Chem.*, **70**, 1943 (1966), have used similar differences in the entropies of activated complexes to suggest inner- and outer-sphere mechanisms for several V^{3+}–MO_2^{2+} reactions.

(29) J. H. Espenson, *Inorg. Chem.*, **7**, 631 (1968).

CONTRIBUTION FROM FRICK CHEMICAL LABORATORY,
PRINCETON UNIVERSITY, PRINCETON, NEW JERSEY 08540

Vibrational Analysis for $Nb_6O_{19}^{8-}$ and $Ta_6O_{19}^{8-}$ and the Raman Intensity Criterion for Metal–Metal Interaction[1a]

BY FRANCIS J. FARRELL,[1b] VICTOR A. MARONI, AND THOMAS G. SPIRO

Received April 3, 1969

Raman and infrared spectra of the octahedral oxyanions $Nb_6O_{19}^{8-}$ and $Ta_6O_{19}^{8-}$ have been subjected to an approximate normal-coordinate analysis. Substantial interaction force constants are required for an adequate fit of the spectra, reflecting the complexity of the force field in these highly condensed complexes. The principal metal–oxygen force constants are quite satisfactory, however, for all three types of oxygen atoms: terminal, bridging, and central. The force constant ratios ~6:3:1 are consistent with a simple bonding scheme in which each oxide ion shares four valence electrons with its neighboring metal ions. As with the structurally analogous $Bi_6(OH)_{12}^{6+}$ a set of cage angles can be replaced in the analysis by a kinetically equivalent set of metal–metal interactions. This internal coordinate is the primary contributor to the lowest frequency A_{1g} fundamental: the "breathing" mode of the metal ions. For $Bi_6(OH)_{12}^{6+}$ this mode produces the most intense band in the Raman spectrum, and metal–metal bonding has been invoked to account for the intensity. For the $M_6O_{19}^{8-}$ complexes, this mode produces one of the weakest Raman bands, consistent with the anticipated absence of metal–metal interaction for these d^0 metal ions. However the "metal–metal" force constants are about the same as for $Bi_6(OH)_{12}^{6+}$. Such force constants evidently have little meaning in bridged polynuclear complexes, and Raman intensity would appear to offer a more reliable criterion for metal–metal interaction.

Introduction

Some years ago Lindqvist and Aronsson showed by X-ray diffraction the existence of discrete polyanions $M_6O_{19}^{8-}$ in crystalline niobates[2] and tantalates.[3] The polynuclear complexes have approximately cubic symmetry, an octahedron of metal atoms being connected by twelve oxygen atoms over the octahedral edges and one in the center of the cage. In addition six peripheral oxygens complete the octahedral coordination shell around each metal. The structure is shown in Figure 1. Alkaline solutions of Nb(V) and Ta(V) also contain hexanuclear anions, as shown by

(1) (a) This investigation was supported by Public Health Service Grant GM-13498, from the National Institute of General Medical Sciences. (b) NIH predoctoral fellow.

(2) I. Lindqvist, *Arkiv Kemi*, **5**, 247 (1953).

(3) I. Lindqvist and B. Aronsson, *ibid.*, **7**, 49 (1954).

light-scattering,[4] ultracentrifugation,[4,5] and potentiometric data.[6] Furthermore the close similarity of crystal and solution Raman spectra[5,7] demonstrates that the cubic structure is retained in solution.

Our interest in these species centers on their structural analogy to $Bi_6(OH)_{12}^{6+}$, which has an octahedron of bismuth ions connected by hydroxyl ions over the octahedral edges.[8] A vibrational analysis for the bismuth complex was recently published.[9a] The most significant finding was that the lowest frequency (<200 cm^{-1}) Raman bands could be assigned almost entirely to motions of the bismuth atoms and these bands were the most intense in the spectrum. Similar results were obtained[9b,c] for the tetrahedral complexes $Pb_4(OH)_4^{4+}$ and $Tl_4(OR)_4$ (R = ethyl and *n*-propyl). On this basis, it was suggested that metal–metal interaction exists in these polyhedral complexes, even though the $5d^{10}6s^2$ valence state of the metal ions is quite stable and their internuclear distances (3.7–3.8 Å) are fairly large.

In this context the $Nb_6O_{19}^{8-}$ and $Ta_6O_{19}^{8-}$ complexes provide reference points for low-frequency Raman intensities. The metal atoms are closer together (3.3 Å) than in $Bi_6(OH)_{12}^{6+}$ but the postulate of metal–metal bonding is implausible because the metal ions have formally a rare gas (d^0) configuration and they also have a full octahedral coordination shell of oxide ions. A glance at the Raman spectra of Aveston and Johnson[5] and of Tobias[7] shows that the bands below 300 cm^{-1} are the weakest in the spectrum, as would be expected if the vibrations responsible for them involve mainly cage deformations. This observation strengthens the inference of bismuth–bismuth bonding in $Bi_6(OH)_{12}^{6+}$. In order to place the comparison on a more quantitative level, we have carried out an approximate vibrational analysis for $Nb_6O_{19}^{8-}$ and $Ta_6O_{19}^{8-}$ which we report here.

Experimental Section

Potassium hexaniobate, $K_8Nb_6O_{19}\cdot 16H_2O$ (Alfa Inorganics), was dissolved in water, filtered through a fine frit, and then recrystallized. Potassium hexatantalate, $K_8Ta_6O_{19}\cdot 16H_2O$, was prepared according to Windmaisser,[10] by fusing K_2CO_3 and TaO_2 in a platinum crucible. The product was dissolved in water, filtered several times through fine pore filters, and recrystallized.

The Raman spectra were recorded on a Cary Model 81 Raman spectrophotometer, using the 4358-Å mercury line for excitation. A standard 7-mm liquid cell was used for the solution spectra. Polarization measurements were made using Polaroid cylinders surrounding the sample tube. The solution samples were filtered through fine pore filters before each spectrum was taken. For crystalline powders a conical sample cell was used.

Infrared measurements were made from 300 to 1000 cm^{-1} with a Beckman IR-12 infrared spectrophotometer. Samples were either mulled in Nujol and pressed between $^1/_{16}$-in. polyethylene windows or else made into KBr pellets.

(4) (a) W. H. Nelson and R. S. Tobias, *Can. J. Chem.*, **42**, 731 (1964); (b) *Inorg. Chem.*, **2**, 985 (1963); (c) *ibid.*, **3**, 653 (1964).
(5) J. Aveston and J. S. Johnson, *ibid.*, **3**, 1051 (1964).
(6) G. Neumann, *Acta Chem. Scand.*, **18**, 278 (1964).
(7) R. S. Tobias, *Can. J. Chem.*, **43**, 1222 (1965).
(8) M. D. Danforth, H. A. Levy, and F. A. Agron, *J. Chem. Phys.*, **31**, 1458 (1959).
(9) (a) V. A. Maroni and T. G. Spiro, *Inorg. Chem.*, **7**, 183 (1968); (b) *ibid.*, **7**, 188 (1968); (c) *ibid.*, **7**, 193 (1968).
(10) F. Windmaisser, *Z. Anorg. Allgem. Chem.*, **248**, 283 (1941).

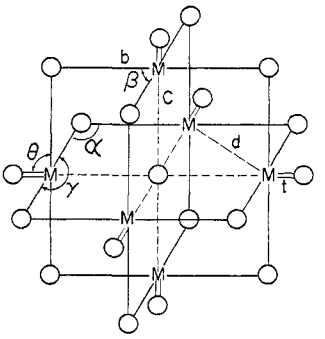

Figure 1.—Structural model for the $M_6O_{19}^{8-}$ ion showing position of metal atoms (M) and oxygen atoms (O). Parameters:[2,3] d = 3.3 Å, b = 2.2 Å, c = 2.35 Å, t = 2.05 Å, α = 106°, γ = 164°, θ = 98°, β = 88°.

Spectral Assignments

Our Raman spectra for $Ta_6O_{19}^{8-}$ and $Nb_6O_{19}^{8-}$, both in crystals and in solution, are in good agreement with those published by Aveston and Johnson[5] and by Tobias.[7] The crystal spectra are better resolved. Their frequencies are listed in Table I. We observed a weak band for $Ta_6O_{19}^{8-}$ at 245 cm^{-1}, not found in the previous studies. It corresponds to the 290-cm^{-1} band of $Nb_6O_{19}^{8-}$, which Tobias[7] also observed. The crystal infrared data, obtained between 300 and 1000 cm^{-1}, are also given in Table I. Our frequencies for $Ta_6O_{19}^{8-}$

TABLE I
OBSERVED AND CALCULATED FREQUENCIES (cm^{-1}) FOR $M_6O_{19}^{8-}$

Species	$Nb_6O_{19}^{8-}$ Obsd	$Nb_6O_{19}^{8-}$ Calcd	$Ta_6O_{19}^{8-}$ Obsd	$Ta_6O_{19}^{8-}$ Calcd
		Raman Bands		
A_{1g}	875	879	860	862
E_g	823	834	832	835
E_g	730	726	740	746
E_g	532	521	520	511
A_{1g}	495	500	475	484
T_{2g}	460	469	415	423
A_{1g}	290	292	245	242
T_{2g}	220	224	215	214
E_g	...	189	...	167
T_{2g}	...	176	...	153
T_{2g}	...	149	...	140
		Infrared Bands		
T_{1u}	856	849	845	845
T_{1u}	685	692	710	711
T_{1u}	523	522	543	539
T_{1u}	414	420	406	411
T_{1u}	...	244	...	203
T_{1u}	...	209	...	191
T_{1u}	...	136	...	134

agree with those reported by Aveston and Johnston,[5] although we did not observe their weak band at 355 cm^{-1}. The infrared spectrum of $Nb_6O_{19}^{8-}$ has not been previously reported. The four bands we observe correspond well with those found for $Ta_6O_{19}^{8-}$.

For $M_6O_{19}^{8-}$ in point group O_h one expects seven infrared-active vibrations, all of T_{1u} symmetry, and eleven Raman-active vibrations classified as: $\Gamma_{Raman} = 3\ A_{1g} + 4\ E_g + 4\ T_{2g}$. For both complexes four infrared and eight Raman bands are ob-

served. Three bands are missing in both the Raman and infrared spectra. In niobate solution Tobias[7] found that the 878- and 290-cm^{-1} Raman bands were polarized. We confirmed this finding and also observed significant polarization for the 495-cm^{-1} shoulder. These three frequencies can be assigned with confidence to the A_{1g} modes of $Nb_6O_{19}^{8-}$. Similarly, in tantalate solution, the 860-, 475-, and 245-cm^{-1} Raman bands are polarized and are of A_{1g} symmetry. The five depolarized Raman bands were assigned to E_g or T_{2g} symmetry (Table I) with the aid of the normal-coordinate analysis (below). The mutual exclusion rule is obeyed, no Raman–infrared coincidence being observed.

Internal coordinates for $M_6O_{19}^{8-}$ are identified in Figure 1. The contributions of each internal coordinate type to the various spectroscopically active symmetry species are listed in Table II. As suggested by Tobias,[7]

TABLE II
SELECTION RULES FOR $M_6O_{19}^{8-}$ SPECIES, POINT GROUP O_h

Internal coordinate (see Figure 1)	No. of modes in each symmetry class									
	A_{1g}	A_{2g}	E_g	T_{1g}	T_{2g}	A_{1u}	A_{2u}	E_u	T_{1u}	T_{2u}
Terminal M–O, t	1	0	1	0	0	0	0	0	1	0
Bridge, M–O, b	1	1	2	1	1	0	0	0	2	2
Central M–O, c	1	0	1	0	0	0	0	0	1	0
M–M, d	1	0	1	0	1	0	0	0	1	1
Terminal O–M–O, θ	1	1	2	1	1	0	0	0	2	2
Bridge O–M–O, β	0	0	1	1	2	0	1	1	2	1
Total	3	1	4	3	4	0	1	1	7	4
Redundancies	2	1	4	0	1	0	0	0	2	2

the high-frequency A_{1g} modes, 878 cm^{-1} for $Nb_6O_{19}^{8-}$ and 860 cm^{-1} for $Ta_6O_{19}^{8-}$, no doubt arise from the in-phase stretching of peripheral M–O bonds. Symmetric (E_g) and asymmetric (T_{1u}) out-of-phase stretching modes are also expected and are readily identified in the spectra at 823 cm^{-1} (Raman) and 856 cm^{-1} (ir) for $Nb_6O_{19}^{8-}$ and at 832 cm^{-1} (Raman) and 845 cm^{-1} (ir) for $Ta_6O_{19}^{8-}$. Below 800 cm^{-1} we expect to encounter stretching modes of the bridging M–O bonds. Stammreich, *et al.*,[11] assigned Raman bands at 558 and 772 cm^{-1} to the symmetric and asymmetric Cr–O–Cr stretches in $Cr_2O_7^{2-}$. The middle-frequency A_{1g} bands, at 495 cm^{-1} for $Nb_6O_{19}^{8-}$ and 475 cm^{-1} for $Ta_6O_{19}^{8-}$, are clearly assignable to the breathing mode of the bridging oxygen atoms. Three other Raman bands are observed for each complex between 400 and 800 cm^{-1} and assigned to the expected T_{2g} and E_g (two) bridge M–O stretching modes. Similarly the two ir bands, at about 530 and 700 cm^{-1}, are assigned to the two expected T_{1u} modes.

The lowest frequency A_{1g} mode, at 290 cm^{-1} for $Nb_6O_{19}^{8-}$ and 245 cm^{-1} for $Ta_6O_{19}^{8-}$, must arise from the breathing mode of the metal atoms (metal and bridge oxygen atoms out of phase). At first we assumed that the restoring force for this motion would be the bond between the metal atoms and the central oxygen atom, but the valence force constant required, about 5 mdyn/Å, is unreasonably high and predicts a central oxygen asymmetric mode (T_{1u}) above 1000 cm^{-1}. A reasonable force constant for this bond, about 1 mdyn/Å, satisfactorily predicts the lowest observed ir band, at 414 cm^{-1} for $Nb_6O_{19}^{8-}$ and 406 cm^{-1} for $Ta_6O_{19}^{8-}$. The predicted symmetric stretch is then below 100 cm^{-1}, so that the restoring force for the observed A_{1g} mode must involve primarily the cage angles α and γ and not the central oxygen. The only feature remaining is the Raman band at 220 cm^{-1} for $Nb_6O_{19}^{8-}$ and 215 cm^{-1} for $Ta_6O_{19}^{8-}$, and this is assigned to terminal M–O bending. In mononuclear transition metal oxyanions the bending modes are usually somewhat higher in frequency.[12] However the angles in these species are tetrahedral and connect equivalent terminal oxygens, which is not the case here. The six fundamentals unaccounted for are primarily deformation modes and can plausibly be situated at frequencies below the detection limits of our instruments.

Normal-Coordinate Analysis

The G matrices were constructed by the method of Wilson, *et al.*,[13] using Schachtschneider's program GMAT.[14] Molecular parameters, shown in the figure, were taken from the X-ray structure determinations. A valence force field was used to construct the F matrix. Both G and F matrices were factored using symmetry coordinates generated from the internal coordinates by standard group theoretical technique.[9a,13] The set of 24 cage angles labeled α and γ in the figure are kinetically equivalent to a set of 12 metal–metal interactions, d. Inasmuch as these coordinates contribute significantly to only one observed mode, namely, the lowest frequency A_{1g} vibration, the metal–metal set was chosen in order to reduce the number of redundancies and also to provide a basis for comparison with the analysis for $Bi_6(OH)_{12}^{6+}$.[9a] Even so the complete set of internal coordinates involve several redundancies, as shown in Table II.

Solution of the secular equations, with least-squares refinement of the force constants, was carried out using Schachtschneider's program FPERT.[14] Initial values of the principal force constants were chosen to place the spectral features in appropriate regions using the assignments discussed above. The only principal force constant which could not be tied down in this way was the one corresponding to the O–M–O angle connecting adjacent bridging oxygens, labeled β in the figure. It is expected to contribute only to low frequencies and was arbitrarily set at a value which calculated the missing frequencies below our detection limits. It did not contribute significantly to the calculation of any of the observed frequencies. Interaction constants were chosen to improve the fit of the calculated frequencies to the observed spectrum.

(11) H. Stammreich, D. Bassi, O. Sala, and H. Siebert, *Spectrochim. Acta*, **13**, 192 (1958).

(12) F. A. Cotton and R. M. Wing, *Inorg. Chem.*, **4**, 867 (1965).

(13) E. B. Wilson, J. C. Decius, and P. C. Cross, "Molecular Vibrations," McGraw-Hill Book Co., Inc., New York, N. Y., 1955.

(14) J. H. Schachtschneider, Technical Reports No. 231-64 and 57-65, Shell Development Co., Emeryville, Calif.

There are of course a large number of interaction constants and also several possible permutations of E_g and T_{2g} assignments in the Raman spectrum. We do not claim to have examined all possibilities. However, among a number of physically reasonable alternatives which were tried, only the one reported here gave an adequate fit to the observed frequencies. The force constants selected and their adjusted values are listed in Table III. The calculated frequencies are compared with the observed values in Table I, while the potential energy distributions are given in Table IV.

TABLE III
ADJUSTED VALENCE FORCE CONSTANTS FOR $M_6O_{19}^{8-}$ (MDYN/Å)

		$Nb_6O_{19}^{8-}$	$Ta_6O_{19}^{8-}$
	Principal Force Constants		
f_t	terminal M–O str	5.66	6.12
f_b	bridge M–O str	2.92	2.94
f_c	central M–O str	0.91	1.30
f_d	M–M str	1.01	1.32
f_θ	terminal O–M–O bend	0.21	0.21
f_β	bridge O–M–O bend at angle β	0.04	0.04
	Interaction Force Constants		
$k_{tt(cis)}$	*cis* terminal str–str	0.10	0.06
$k_{bb(\alpha)}$	bridge str–str at angle α	−0.09	−0.19
$k_{bb(\beta)}$	bridge str–str at angle β	−0.22	−0.12
$k_{bb(\gamma)}$	bridge str–str at angle γ	0.60	0.65
k_{bc}	bridge str–central str	0.20	0.34
$k_{b\theta}$	bridge str–terminal bend for adjacent b and θ	0.33	0.40

Discussion

The potential energy distributions show that the internal coordinates are fairly well separated in the normal modes and that the assignments are reasonable. The three bands above 800 cm^{-1} are almost pure terminal M–O stretching. The bands between 800 and 400 cm^{-1} are mainly bridge M–O stretching, except that the lower two infrared modes have large contributions from central oxygen motions. The lowest frequency Raman band is mostly terminal M–O deformation, while the lowest of the three A_{1g} modes has a predominant contribution from the "metal–metal" coordinate, *i.e.*, cage deformations. The six unobserved bands, calculated at low frequency, are mixed deformation modes with some stretching contributions.

A total of 11 adjustable force constants (f_β is fixed arbitrarily) were required to obtain an adequate fit to the 12 observed frequencies. Some of the interaction constants are quite large, as was also found for $Bi_6(OH)_{12}^{6+}$. We feel that they simply express the inadequacy of a conventional valence force field for such highly condensed complexes and attach no significance to their values. It should be noted however that an interaction constant between the terminal M–O stretches is required to account for the noncoincidence of the highest frequency A_{1g} and E_g bands. The diagonal G matrix elements are identical for these two modes, and mixing with other coordinates is slight, yet they are well spread apart in frequency. Since the terminal oxygens are spatially well separated, the phenomenon suggests, surprisingly, transmission of electronic effects through intervening metal and bridging oxygen atoms. The interaction constant is substantially smaller than it is for two terminal M–O stretches on the same metal in a number of oxy–transition metal complexes.[12]

TABLE IV
POTENTIAL ENERGY DISTRIBUTION

Normal mode freq, cm^{-1}	V_{tt}[a]	V_{bb}	V_{cc}	V_{dd}	$V_{\theta\theta}$	$V_{\beta\beta}$	V_{bc}	$V_{b\theta}$
				$Nb_6O_{19}^{2-}$				
875 (A_{1g})	97.0	0	0	1.8	0	0	0	0
856 (T_{1u})	95.6	0.9	0.9	1.0	0.5	0	0.4	0
823 (E_g)	94.0	2.6	0.4	0	1.0	0	0.4	1.1
730 (E_g)	4.8	78.0	0	0	3.9	0	0	13.1
685 (T_{1u})	2.4	72.1	1.7	0	4.6	0	4.1	15.1
532 (E_g)	0	115.4	0	0	8.9	0	0.5	−25.0
523 (T_{1u})	0.7	87.9	14.6	2.8	5.5	0	7.7	−19.4
495 (A_{1g})	0	112.4	0	1.0	7.2	0	2.2	−23.5
460 (T_{2g})	0	119.9	0	6.1	12.3	0	0	−38.8
414 (T_{1u})	0.3	42.3	87.3	0	6.2	0	−23.5	−12.6
290 (A_{1g})	2.2	8.0	15.0	66.9	24.2	0	−5.4	−12.1
244 (T_{1u})	0.8	12.9	0.1	62.9	36.9	3.4	0.5	−17.6
220 (T_{2g})	0	4.4	0	1.0	117.4	0	0	−22.9
209 (T_{1u})	0	17.3	1.1	6.2	110.5	0	−0.7	−25.0
189 (E_g)	1.0	16.7	37.9	42.0	30.3	0	−11.1	−16.9
176 (T_{2g})	0	6.2	0	40.4	3.1	54.8	0	−4.5
149 (T_{2g})	0	3.6	0	46.7	1.3	50.6	0	−2.2
136 (T_{1u})	0	1.2	0	2.0	2.0	96.2	0	−1.5
				$Ta_6O_{19}^{8-}$				
860 (A_{1g})	98.9	0	0	0.7	0	0	0	0
845 (T_{1u})	97.5	0.5	0.7	0.4	0.2	0	0.4	0.3
832 (E_g)	97.0	1.5	0.2	0	0.3	0	0.3	0.6
740 (E_g)	2.6	77.6	0	0	3.8	0	0.5	15.5
710 (T_{1u})	1.9	56.4	9.1	0	4.5	0	13.0	15.0
543 (T_{1u})	0.2	42.2	52.6	0.7	2.4	0	0.6	1.2
520 (E_g)	0	121.6	0	0	9.3	0	0.8	−31.8
475 (A_{1g})	0.3	118.5	0	0.9	8.1	0	3.4	−31.4
415 (T_{2g})	0	128.4	0	2.8	8.4	0	0	−39.8
406 (T_{1u})	0	114.2	50.8	0.4	9.6	0	−40.2	−34.8
245 (A_{1g})	0.8	16.5	18	72.5	23.9	0	−11.7	−20.1
215 (T_{2g})	0	22.3	0	1.4	144.8	0	0	−68.7
203 (T_{1u})	0.2	21.4	0.6	65.0	41.6	4.3	−1.9	−31.6
191 (T_{1u})	0.1	31.3	0.2	12.0	124.9	0	0	−68.5
167 (T_{2g})	0	1.9	0	14.1	1.5	84.5	0	−2.0
153 (E_g)	0.3	24.4	46.9	47.1	26.9	0	−21.8	−24.0
140 (T_{2g})	0	4.8	0	77.1	2.7	19.7	0	−4.3
134 (T_{1u})	0	1.2	0	3.0	1.7	95.7	0	−1.6

[a] V_{ij} is the normalized contribution to the potential energy from F matrix elements of the type (i,j).

The principal force constants for M–O stretching are quite satisfactory. The terminal stretching constant for $Nb_6O_{19}^{8-}$ is the same as the Mo–O stretching constant in oxy complexes of the isoelectronic Mo(VI):[12] MoO_4^{2-} and MO_3·dien. Cotton and Wing[12] have assigned an M–O bond order of two for these species. For both $Nb_6O_{19}^{8-}$ and $Ta_6O_{19}^{8-}$ the ratios of terminal to bridging to central M–O stretching constants are not far from 6:3:1. This is consistent with a simple bonding picture in which each of the oxide ions shares four valence electrons with its neighboring metal atoms. Average M–O bond orders would be 2, 1, and $^1/_3$ for terminal, bridging, and central oxygen atoms, respectively. These differences would be expected to be reflected in the M–O bond distances as well, but the oxygen atoms were not accurately located in the X-ray structure analysis. The principal bending force constants are difficult to assess, but their values seem not unreasonable.

We consider, finally, the "metal–metal" force constant, which, at ~1 mdyn/Å, is sizable. In fact it is slightly larger than in $Bi_6(OH)_{12}^{6+}$.[9a] For both $M_6O_{19}^{8-}$ and $Bi_6(OH)_{12}^{6+}$ the set of "metal–metal" coordinates is kinetically equivalent to the set of cage angles α and γ. In both cases the "metal–metal" coordinate is the main contributor to the lowest frequency A_{1g} fundamental. However while this fundamental gives the strongest Raman band in the $Bi_6(OH)_{12}^{6+}$ spectrum, it gives one of the weakest for $Nb_6O_{19}^{8-}$ and $Ta_6O_{19}^{8-}$. In the Wolkenstein bond polarizability theory,[15] Raman intensity for totally symmetric vibrations of isotropic molecules arises exclusively from the stretching of bonds; bond bending does not contribute. This assumption has been tested experimentally and holds rather well.[16–18] The low intensity observed for the M_6 breathing mode for the $M_6O_{19}^{8-}$ species can be attributed to the small admixture of bridge and central oxygen stretching. The high intensity observed for $Bi_6(OH)_{12}^{6+}$, on the other hand, suggests that metal–metal interaction is significant.

It does not follow, however, that the "metal–metal" force constant for $Bi_6(OH)_{12}^{6+}$, 0.97 mdyn/Å,[9a] is a realistic reflection of the strength of the interaction. The present study shows that one can obtain force constants of this magnitude without any metal–metal interaction. The restoring force arises from the kinetically equivalent set of cage deformations. No doubt this is the case for $Bi_6(OH)_{12}^{6+}$ as well, since it seems highly unlikely that the Bi–Bi "bond" could be as strong as the metal–metal bonds in $Re_2(CO)_{10}$ or $Mn_2(CO)_{10}$, for which the metal–metal force constants are 0.82 and 0.59 mdyn/Å, respectively.[19] These considerations emphasize the primacy of Raman intensities over vibrational frequencies in any discussion of metal–metal bonding in polynuclear complexes with bridging ligands.

(15) M. Wolkenstein, *Dokl. Akad. Nauk SSSR*, **30**, 791 (1941).
(16) D. A. Long, A. H. S. Matterson, and L. A. Woodward, *Proc. Roy. Soc.* (London), **A224**, 33 (1954).
(17) G. W. Chantry and R. A. Plane, *J. Chem. Phys.*, **35**, 1027 (1961).
(18) G. W. Chantry and R. A. Plane, *ibid.*, **34**, 1268 (1961).
(19) C. O. Quicksall and T. G. Spiro, *Inorg. Chem.*, **8**, 2363 (1969).

CONTRIBUTION FROM THE DEPARTMENT OF CHEMISTRY OF THE UNIVERSITY OF CALIFORNIA AND THE INORGANIC MATERIALS RESEARCH AND NUCLEAR CHEMISTRY DIVISIONS OF THE LAWRENCE RADIATION LABORATORY, BERKELEY, CALIFORNIA 94720

Nitrogen 1s Electron Binding Energies. Correlations with Molecular Orbital Calculated Nitrogen Charges

By DAVID N. HENDRICKSON,[1] JACK M. HOLLANDER,[2] AND WILLIAM L. JOLLY[1]

Received May 30, 1969

Nitrogen 1s electron binding energies are given for 56 nitrogen compounds. Correlations are observed between these measured binding energies and nitrogen atom charges calculated from either CNDO or extended Hückel molecular orbitals. The molecular structure of the oxyhyponitrite ion ($N_2O_3^{2-}$) and the bonding characteristics of various metal-coordinated ligands are investigated by means of these correlations.

Introduction

Extensive studies of chemical shifts associated with atomic core electron binding energies have been made by Siegbahn *et al.*,[3] by use of the relatively new technique X-ray photoelectron spectroscopy. Measured binding energies have been correlated with formal oxidation states and with fractional atomic charges calculated by a modification of Pauling's method. We have recently reported preliminary results of a study of solid nitrogen compounds by X-ray photoelectron spectroscopy, and we have shown that the nitrogen 1s binding energies can be correlated with nitrogen atomic charges calculated from CNDO molecular orbital eigenfunctions.[4]

In this paper we extend the correlation of the nitrogen 1s binding energy data to include atomic charges evaluated by the extended Hückel molecular orbital method. We use these correlations and the observed nitrogen 1s binding energies for sodium oxyhyponitrite ($Na_2N_2O_3$) to establish the structure of the $N_2O_3^{2-}$ ion. In addition, we use binding energy data for some nitrogen-containing metal-coordinated ligands to characterize the bonding in these ligands.

Experimental Section

Mg Kα X-radiation (1253.6 eV) was used. The kinetic energy of the photoelectrons was measured in an iron-free, double-focusing magnetic spectrometer[5] shown schematically in Figure 1. The instrumental line width, including the contribution from the X-ray line, was about 1 eV, and the observed photoelectron lines had widths of 1.5–2.5 eV. Photoelectrons were counted[6] typi-

(1) Department of Chemistry, University of California, and Inorganic Materials Research Division, Lawrence Radiation Laboratory, Berkeley, Calif.
(2) Nuclear Chemistry Division, Lawrence Radiation Laboratory, Berkeley, Calif.
(3) K. Siegbahn, C. Nordling, A. Fahlman, R. Nordberg, K. Hamrin, J. Hedman, G. Johansson, T. Bergmark, S.-E. Karlsson, I. Lindgren, and B. Lindberg, "ESCA Atomic Molecular and Solid State Structure Studied by Means of Electron Spectroscopy," Almqvist and Wiksells AB, Uppsala, 1967.
(4) J. M. Hollander, D. N. Hendrickson, and W. L. Jolly, *J. Chem. Phys.*, **49**, 3315 (1968), and references therein.
(5) J. M. Hollander, M. D. Holtz, T. Novakov, and R. L. Graham, *Arkiv Fysik*, **28**, 375 (1965); T. Yamazaki and J. M. Hollander, *Nucl. Phys.*, **84**, 505 (1966).
(6) A Bendiz curved channel multiplier ("Channeltron") was used as the electron detector.